
Enhanced-image-quality raster-scanning chipset using feedback-control actuation

Sharon Hornstein
Tal Langer
Tsur Assis
Arnon Hirshberg

Abstract — A new raster-scanning chipset which provides enhanced projection performance is presented. The design is novel in that it combines electrostatic and electromagnetic actuation methods, along with a unique feedback-control scheme to produce SVGA and WVGA projected images. A micromirror, the actuators, and drive electronics are integrated into a small, power-efficient system, a scanning chipset, to increase its reliability and manufacturability.

Keywords — Projection displays, scanning, MEMS.

DOI # 10.1889/JSID18.10.862

1 Introduction

The growing usage of mobile devices along with the progress in their capabilities has opened up new possibilities for the mobile world. The availability of rich multimedia with endless colorful content, in addition to all-time connectivity, expanded the use of mobile devices from personal viewing into multimedia working and sharing platforms, both for business users and entertainment consumers. However, as the applications of mobile devices have become more sophisticated, and due to the dramatic increase of their variety, new standards and ambitious demands have emerged. Above all, power consumption and the physical size of these devices are the most crucial needs. Consequently, new constraints regarding designing new hardware components for the mobile world have arisen, giving raise to the appearance of miniature projection systems.

Several solutions^{1,2} have been suggested to address demands for such miniature systems. However, none has provided an overall satisfying solution. Tradeoffs between power consumption (for LCD, DLP, DMD, or LCoS solutions³⁻⁵) and the quality of projection (for other MEMS scanning devices) have been proposed; yet, none of those seems to have a winning ticket. Conant *et al.*² demonstrated the feasibility of micro-machined raster-scanning displays for video images, but pointed out that improvements in mirror resonant frequency and mirror stiffness are necessary to display VGA-quality video. Urey⁶ has compared scanning schemas resolution and limitations. Schreiber *et al.*⁷ and Brown *et al.*⁸ presented Lissajous-like scanning solutions. Various actuation schemes^{5,9-13} have been developed to drive a two-axes scanning mirror. Sprague *et al.*¹⁴ have been using a coupled electromagnetic drive, which results in a SXGA resolution. Kwon *et al.*¹⁵ have implemented a new isolation method for a two-dimensional gimbaled micromirror. Du *et al.*¹⁶ designed and fabricated a 2-D in-plane diffraction grating scanner with an optical scan angle of 5.2°, which they admit that their scanner has a lower scan angle than other micro-scanners.

Maradin's scanning micromirror is based on a gimbaled MEMS structure with two uncoupled actuators for

the horizontal and vertical directions. The horizontal scan is based on an electrostatic resonating actuator driven by a comb structure, whereas the vertical scan is driven by electromagnetic forces generated by a set of micro-coils and a rotating magnet. This combination of two different actuation mechanisms offers several advantages over the conventional MEMS scanning micromirrors. It minimizes the cross-coupling between two axes of scanning motion, requires low driving power, increases deflection angle, and improves the resolution of position sensors.

In the presently reported work, the novel design of the two-dimensional MEMS scanning micromirror is presented to enhance image quality by using feedback-control actuation. This Maradin design enables high-resolution images (WVGA/SVGA and up) interlaced or progressive, without scanning distortions at high optical efficiency for low-power laser-projection solutions.

2 Scanner architecture

Maradin's scanning chipset¹⁷ is an electromechanical system that is composed of three main parts: a scanning element, an electromagnetic actuator, and an electronic driver. These three units are assembled together in an optical chamber to form a miniature component, herein termed a "scanning chipset" not bigger than 0.4 cm³. Figure 1 depicts a schematic sketch of Maradin's chipset. The scanning element is based on a two-degrees-of-freedom (DoF) MEMS gimbaled mirror with each axis actuated independently. The horizontal direction, customarily referring to the greatest image dimension (with the larger number of pixels), is parallel to the interpupillary axis. The vertical direction, customarily refers to the smaller image dimension (with the smallest number of pixels), is parallel to the gravity vector. The horizontal axis is driven by an electrostatic resonating actuator based on a vertical comb drive (VCD).¹⁸ The vertical axis utilizes an electromagnetic actuator based on a micro-version of a limited magnetic torque (LMT) motor with rotating magnets.

The authors are with Maradin Technologies, Ltd., 2 HaCarmel St., Yokneam, Israel 37023; telephone +972-4637-1598, e-mail: Sharon.h@maradin.co.il.
© Copyright 2010 Society for Information Display 1071-0922/10/1810-0862\$1.00.

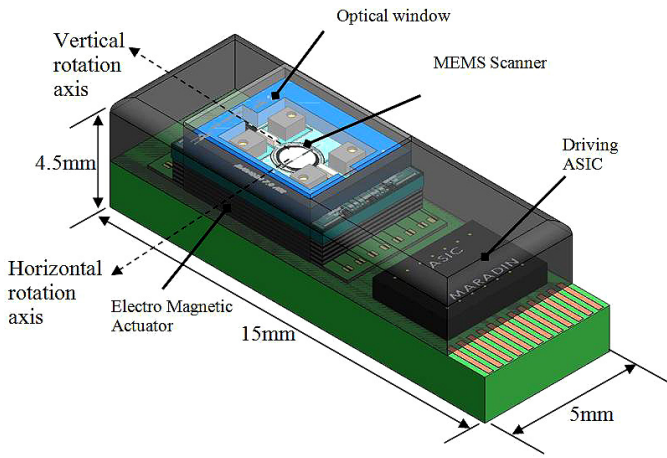


FIGURE 1 — Schematic sketch of the MEMS scanner.

We note that the use of two different actuation concepts for each DoF decouples the electromechanical response of the system, which results in reduced optical distortions and simplification of the MEMS design and its implementation. Moreover, a progressive design of the micro-coils that are used for the electromagnetic forcing of the vertical scan enables an increase in vertical angle, without the need to modify the mechanical design of the component.

The scanning method chosen for the projecting process of the image is based on a raster-scanning pattern, which is built up from two interlaced fields. This procedure is similar to common CRT television scanning and is used by other devices for display. Although scanning technology for television was changed with the transition to flat panels, mainly since flat panels cannot support interlacing, flickering effects were solved by means of an increase of the refreshment rate. However, a true raster interlaced scan, especially for a wide range of miniature projection applications, enables maintaining a lower refreshment frequency, which allows much more flexibility of the design. Consequently, Maradin's scanning pattern utilizes a bi-directional scan, which eliminates the need for line retrace, and therefore is time efficient and enables an enhanced quality image. The meaning of a bi-directional scanning is that each second line of the image is inversely projected (*i.e.*, if the first line is projected from left to right, the second line is projected from right to left, and vice-versa). Realization of this solution requires an additional memory unit, which is part of the electronic unit of the device.

One of the novelties of the presented design is its ability to scan a straight row, which results in a uniform row-to-row spacing, as illustrated in Fig. 2. This solution is fundamentally different from current state-of-the-art scanners and CRT televisions, in which projection is performed at an angle (rather than a straight line). Consequently, Maradin's concept for scanning requires half of the resonant frequency needed to create the image, and the light-source utilization is doubled with respect to state-of-the-art scanners,¹⁹ which allows similar angular performances at lower

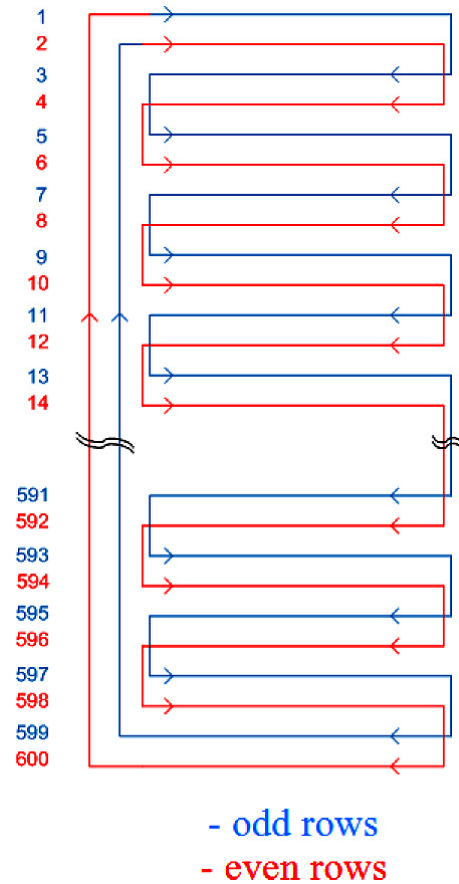


FIGURE 2 — Straight row interlaced raster scanning. The blue line represents the odd field and the red line represents the even field.

power consumption. Finally, the use of a staircase waveform in the vertical axis guarantees that the spacing between the scanned horizontal lines is constant and the lines are parallel. This reduces geometrical distortion and leads to better image quality.

The vertical scan is made of two sequential sawtooth signals, which include interlaced odd and even fields. Each

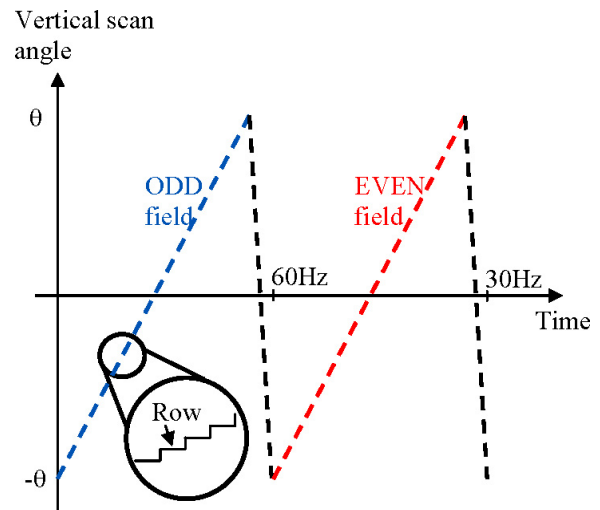


FIGURE 3 — Vertical scan sawtooth profile. Each ramp sequentially represents even and odd fields. The ramp contains staircase steps where each step corresponds to a straight horizontal row.

TABLE 1 — Scanner performance: geometrical and physical parameters.

Parameter	Description	Value
Resolution	Projection resolution	WVGA/SVGA
N_h	Horizontal resolution	854/800
N_v	Vertical resolution	480/600
D	Mirror size (horizontal axis)	1100 μm
D'	Mirror size (vertical axis)	1000 μm
F_r	Frame scanning rate	30 Hz
K_{sp}	Spot size to pixel size ratio	1
K_{os_h}	Horizontal over scan constant	0.9
K_{os_v}	Vertical over scan constant	0.9
K_T	Beam clipping constant	1.14
Λ	Wavelength (color red)	0.632 μm
K_{ub}	Scan directions (bidirectional)	2
A	Beam-Mirror impinge angle (horizontal)	20°
a	Shape factor of mirror (ellipse)	1.06

sawtooth ramp consists of a staircase-step profile as illustrated in Fig. 3. Each step represents a row in the field. The straight row is achieved by a feedback control over the mirror position sensor.

3 Scanner system architecture

The MEMS scanner is designed to project a WVGA/SVGA image at a 30-Hz refresh rate (interlaced). Both 4:3 and 16:9 image ratios are possible via a proper design of the electronic circuit that controls the light sources. The scanner performance is derived from resolution criteria. Table 1 comprises the geometrical and physical parameters of the scanner according to Ref. 19.

By using the constants from Table 1 and describing the desired resolution and optical beam profile, we calculate the maximum mechanical scan angles (MMSA) as:

$$\theta_{MMSA} = \frac{N_h K_T a \lambda}{4DK_{sp}K_{os_h} \cos\alpha} \cong 10^\circ, \quad (1)$$

$$\theta'_{MMSA} = \frac{N_v K_T a \lambda}{4D'K_{sp}K_{os_h}} \cong 6.88^\circ. \quad (2)$$

Note that θ_{MMSA} is the horizontal required scan angle whereas θ'_{MMSA} is the vertical required scan angle.

Laser-architecture requirements include a continuous-wave, circular, 0.6-mm-waist beam laser. The power consumption for the laser is limited to several hundreds of milliwatts. The speckles issue is currently not addressed because it is handled by the laser manufacturer. However, future work regarding this issue is planned as part of the scanner design to assure a high-quality projected image.

4 Horizontal axis

The horizontal scanning direction, which refers to lines for interlaced scan, is achieved by the oscillation of the MEMS micromirror at its resonance frequency. The micromirror is driven via an electrostatic resonating actuator based on a vertical comb structure that is inherently fabricated using

MEMS technology, along the rotational axis. The excitation frequency is designed to be a function of both the required resolution (*e.g.*, 800 pixels) and the required frame rate (*i.e.*, vertical scanning rate).

In order to evaluate the horizontal scan rate, the following formation is used¹⁹:

$$f_s = \frac{F_r N_v}{K_{os_v} K_{ub}} = 10 \text{ kHz}. \quad (3)$$

The fabrication process of the device creates variations over the geometrical and physical properties on each die, and also between components that are located on the same wafer. The working environment, such as temperature, pressure, and humidity also affect the silicon properties. Therefore, each MEMS component may have a slightly different resonance frequency. Consequently, a dedicated driver is used to track each device's resonance frequency. The frequency is deduced from a capacitance position sensor implemented inherently in the horizontal electrostatic comb. The sensor is connected to a control loop in parallel to the driving circuit. A PLL feedback is used to lock the system on the actual resonant frequency. Operation at resonant frequency takes advantage of the high damping factor (Q) and achieves high angular performance at low energy. Furthermore, synchronizing the video signals with the modulated image is made possible via a frequency-locking procedure and overcomes the minor frequency changes.

In order to achieve a super-video-graphics-array (SVGA) image, via a resolution of 600 × 800 pixels and a frame rate of 30 Hz, it is required to obtain both a large deflection angle as well as a high-resonating frequency. Therefore, a closed-loop control for the horizontal direction is used. Figure 4 depicts a schematic block diagram that includes the main features of the system: the MEMS micromirror, its driver, a digital-to-analog converter (DAC), and the frequency analyzer (PLL). A capacitive rotational position sensor is used in the feedback-control loop, generating the change in its capacitance as the MEMS moves. Consequently, a high-resolution capacitive readout circuit is required to detect the position information of the MEMS. Realization of the horizontal-position sensor is performed by a comb structure, the same one that is used for the electrostatic actuation.

In order to obtain a large enough deflection angle, an 80-V driving voltage is required to generate the sufficient electrostatic torque for the mirror. This voltage is generated

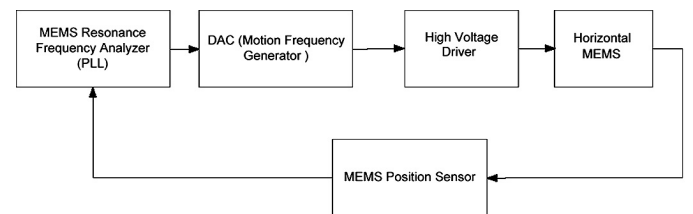


FIGURE 4 — Control block diagram illustrating the horizontal scanning.

by dual-stage boost converter circuits that are located in the ASIC.

Vibrating the mirror in the horizontal direction is achieved by a sine-wave voltage signal that controls the mirror. Due to the non-uniform characteristic of the sine profile, the scanning speed across the row is uneven. This yields pixel smearing and consequently a distorted image. To overcome this problem, Maradin's chipset design includes laser modulation that varies according to the row position.²⁰

5 Vertical axis

The vertical scanning direction, which refers to the projected columns, is modeled as a torsional spring-inertia system. The system is excited by a time-varying torque $T(t)$, which is produced by the magnetic motor, composed of a set of micro-coils and a permanent rotating magnet, located on both sides of the micromirror. A magnetic core, located at the basis of the chipset (see Fig. 1) and separated by an air gap from the mirror, is magnetically actuated using a set of field coils. Current flow in the field coils generates a magnetic field in the air gap, which interacts with the magnetic moment of the permanent magnet. This produces a reciprocating torque in the axis of the permanent magnet, thus enabling its rotation. There are a total of four coils, arranged in pairs, each two located close to the boundaries of the vertical axis. As each pair of coils enables the rotation at the end of the axis, the other pair of the coils, working at the other end, increases the torque in the system.

This unique electromagnetic design simplifies the fabrication process of the mechanical component by means of its design. The mechanical system is designed such that its inertia is minimal and its driving components are manufactured separately, and are assembled externally (*i.e.*, on the mounting of the chipset rather than on the rotating elements). Consequently, a small inertia contributes to large scan angles and enables scalability of the image. The external driving components can be designed separately and con-

trol the performance of the chipset, without the need to alter the mechanical design.

The torque produced in the motor is proportional to the current flowing in the coil. This torque is opposed by the friction and the spring constant of the supporting torsional springs. Thus, the equivalent mechanical model can be described as

$$J_{xx}\ddot{\theta} + D\dot{\theta} + K\theta = K_T \cdot i(t), \quad (4)$$

where J_{xx} is the moment of inertia, D is the damping coefficient, K is the spring constant, and K_T is the torque constant of the magnetic motor. Likewise, $i(t)$ is the input current to the system and θ is the angular rotation.

In order to achieve Maradin's bi-directional advantage of the straight horizontal scan and row-to-row uniform spacing, a high-performance controlled magnetic actuator is used. A current-loop feedback control, designed as an inner loop as part of a comprehensive position loop, is used to preserve the mirror position.

Current loop: The vertical position of the mirror is determined according to the current that drives the device. We define the resolution of the vertical scanning as 1/8 pixel. In order to define the current-loop bandwidth, we multiply the number of rows by the scanning frequency, which yields 144 kHz. The bandwidth is chosen such that it is wider than the required frequency, and hence we set the loop bandwidth to 1 MHz. This will guarantee a stable current, which assures that the vertical position of the mirror is kept at its desired position.

Vertical position sensor: The MEMS is designed such that it comprises of position sensors along the vertical rotation axis, based on a comb structure that is inherently fabricated using MEMS technology. The sensors are based on the capacitance changes when the MEMS is rotated around its longitudinal axis. In order to facilitate the capacitance sensing, a high-frequency term is added to the excitation voltage.²¹

The vertical angular sensor is designed to have a linear sensitivity in the range of $\pm 15^\circ$ mechanical angle. The sensor

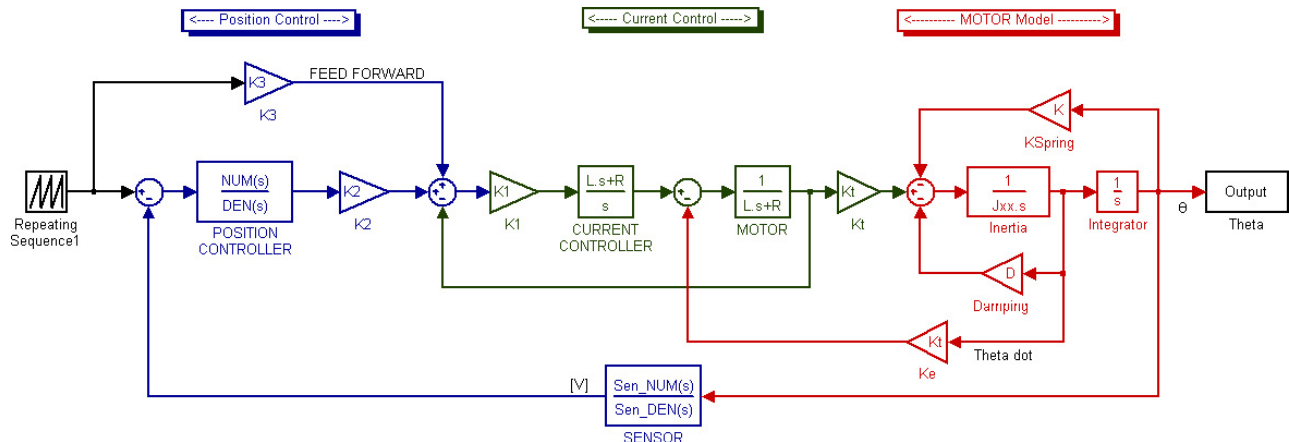


FIGURE 5 — Vertical-axis feedback-control-drive block diagram for a sawtooth profile.

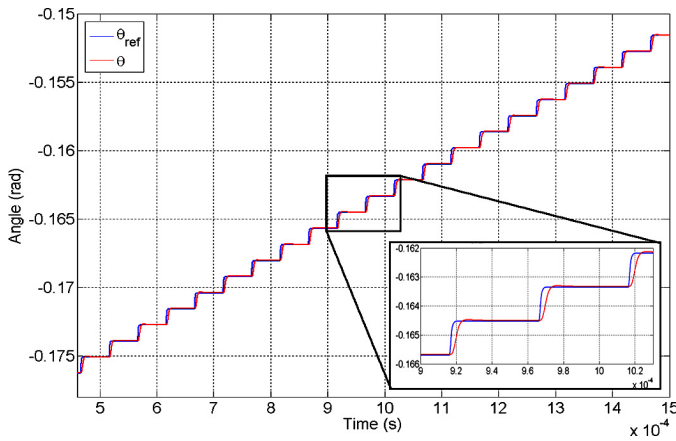


FIGURE 6 — Gimballed angular position: the vertical axis of the gimbal (red line) compared to the sawtooth profile input (blue line). Each step corresponds to a straight horizontal row.

range is more than twice the required θ'_{MMSA} [Eq. (2)]. To satisfy the 1/8-pixel vertical resolution we calculate the required angular sensitivity:

$$\text{Sens}_v = \frac{2\theta'_{MMSA}}{N_v \cdot 8} = 2.8 \times 10^{-3} \text{ (deg)}. \quad (5)$$

Based on a horizontal scanning frequency of 10 kHz, scanning of a single line takes $1/(10 \times 2) \text{ kHz} = 50 \mu\text{sec}$ (as of bi-directional scanning). We excite the system using a sine wave and assume an efficiency of 0.9. Therefore, the practical time for one line is $45 \mu\text{sec}$. We allow a settling time of $5 \mu\text{sec}$ for the system to converge to 95% of the steady-state value of each step. We use the settling time as an estimate for the minimum required sampling rate, and set it as 500 kHz. The angular position, measured by this sensor, is used in the feedback loop for the vertical torsional dynamics. Figure 5 depicts the block diagram of the Gimbal's vertical axis. The block diagram is composed of three parts: the dynamical system, a current-loop control, and the position loop.

Simulation results: For an image resolution of 600 × 800 pixels and a frame rate of 30 Hz, the frame is decomposed into two fields. Each field is comprised of 300 rows and has a field rate of 60 Hz. Thus, each field projection will

take 16.6 msec. The transition of one row to the next one is designed such that it takes less than $5 \mu\text{sec}$.

Figure 6 represents a simulation result of the system. The input of the system in the vertical scanning direction is a sawtooth signal that is composed of a repeating sequence of 300 steps. The detailed view in the bottom right of Fig. 6 depicts two lines; the system response (red curve) is drawn next to the reference signal (blue line). Two important system characteristics can be identified. The system's rise time can be approximated as $6.4 \mu\text{sec}$ and its settling time is approximately $13.4 \mu\text{sec}$, which is the time needed for stabilizing the row such that it is maintained at its position without oscillations.

Experimental results: The control system was also tested for a working chipset. A 10-mV step was given to the position reference and the sensed position is observed, as shown in Fig. 7 (left). The voltage reference and the actual voltage across the MEMS is also shown in the figure. It is seen that the position reaches the desired position in about $12 \mu\text{sec}$ and results in a voltage overshoot of 4 V due to the slow rate of the current in the inductor.

The chipset was also tested on a position reference pattern emulating a complete field (Fig. 7, right). The field is comprised of 300 rows with a dynamic range of 0.15–1.65 V and spanning of 16.6 msec.

Figure 8 demonstrates a 2-D picture of the chipset (currently, a single red laser is used).

6 Conclusion

A novel microscanner, based on a micromirror supported by two uncoupled rotational axes, has been developed. The design meets the needs of a high-resolution display and manages to significantly reduce the size and power consumption of the device. A novel feedback-control system enables a high-quality image, which compensates variations of physical and geometric properties due to fabrication and environmental effects.

The Maradin novel design of the two-dimensional MEMS scanning micromirror implements several innovative solutions in the field of actuation and control of scan-

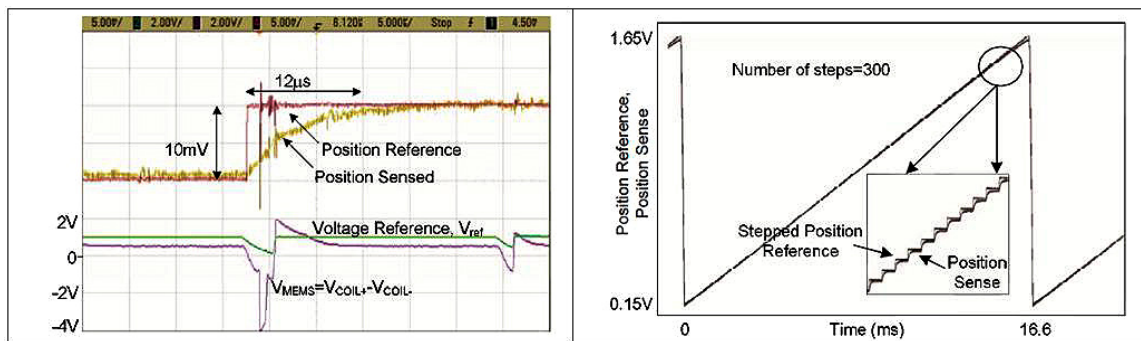


FIGURE 7 — Experimental results using the chipset. Left: the output response of the overall scheme with a 10-mV step change in the position reference. Right: The closed-loop system showing the position reference and the actual sensed position for one field.



FIGURE 8 — Demonstration of a working projecting system at Maradin's lab.

ning micromirrors. These novelties enable a *SVGA resolution* with both *interlaced and progressive scanning* regimes to eliminate inherent scanning distortions and to utilize a high-optical-efficiency solution of laser projection for overall system power efficiency.

References

- 1 W. Makishi *et al.*, "Magnetic torque driving 2-D micro scanner with a non-resonant large scan angle," *Transducers 2009*, June 21–25, Denver, CO, U.S.A. (2009).
- 2 R. A. Conant *et al.*, "A raster-scanning full motion video display using polysilicon micromachined mirrors," *Transducers '99*, The 10th International Conference on Solid-State Sensors and Actuators, June 7–10, Sendai, Japan (1999).
- 3 L. J. Hornbeck, "Digital light processing for high-brightness, high-resolution applications," *Electronic Imaging, EI '97, Projection Displays III*, February 10–12, San Jose, CA (1997).
- 4 P. F. van-Kessel *et al.*, "A MEMS-based projection display," *Proc. IEEE* **86**(8) (1998).
- 5 C. D. Liao and J. C. Tsai, "The evolution of MEMS displays," *IEEE Trans. Industrial Electron.* **56**(4) (2009).
- 6 H. Urey, "Bi-axial magnetic drive for scanned beam display mirrors," *Proc. SPIE* **4773**, 27–37 (2002).
- 7 P. Schreiber *et al.*, "Laser display with single-mirror MEMS scanner," SID Spring Meeting, March 13–14, Jena, Germany (2008).
- 8 M. Brown *et al.*, "Image quality considerations in bi-sinusoidally scanned retinal scanning display systems," *SID Symposium Digest* **33**, 212 (2002).
- 9 H. Schenk *et al.*, U.S. Patent 6595055 (2003).
- 10 M. Fisher *et al.*, "Electrically deflectable polysilicone micromirrors—dynamic behavior and comparison with the results from FEM modeling with ANSYS," *Sensors and Actuators A: Physical* **67**, 89–95 (1998).
- 11 S. Oak *et al.*, "Rotating out-of-plane micromirror," *J. Microelectromechanical System* **19**(3) (2010).
- 12 S. H. Sadat *et al.*, "Large-deflection spiral-shaped micromirror actuator," *J. Microelectromechanical System* **18**(6) (2009).
- 13 A. D. Yalcinkaya *et al.*, "Two-axis electromagnetic microscanner for high resolution displays," *J. Microelectromechanical System* **15**(4) (2006).
- 14 R. Sprague *et al.*, "Bi-axial magnetic drive for scanned beam display mirrors," *Proc. SPIE* **5721**, 1–13 (2005).
- 15 S. Kwon *et al.*, "Vertical comb-drive based 2-D gimbaled micromirrors with large static rotation by backside island isolation," *J. Selected Topics in Quantum Electron.* **10**(3), 498–504 (2004).
- 16 Y. Du *et al.*, "High speed laser scanning using MEMS driven in-plane vibratory grating: Design, modeling and fabrication," *Sensors and Actuators A: Physical* **156**, 134–144 (2009).
- 17 Y. Lubianiker *et al.*, "Gimbaled scanning micro-mirror apparatus," PCT/IL2008/000743 (2009).
- 18 O. Solgaard *et al.*, "Self aligned vertical electrostatic comb-drives for micromirror actuation," *JMEMS* **12**, 458–464 (2003).
- 19 D. Armitage *et al.*, *Introduction to Microdisplays* (Wiley, 2006).
- 20 H. Urey *et al.*, "Optical performance requirements for MEMS-scanner based microdisplays," *Proc. SPIE* **4178**, 176–185 (2000).
- 21 S. Y. Peng *et al.*, "A charge-based low-power high-SNR capacitive sensing interface circuit," *IEEE Trans. Circuits Systems-I: Regular Papers* **55**(7) (2008).